Electronic structure of molecular icosahedra films

1995 J. Phys.: Condens. Matter 7 7185

(http://iopscience.iop.org/0953-8984/7/36/008)

J. Phys.: Condens. Matter 7 (1995) 7185–7194. Printed in the UK

Electronic structure of molecular icosahedra films

Jiandi Zhang†, D N McIlroy†, P A Dowben†, Hong Zeng‡, G Vidali‡, D Heskett§ and M Onellion‖

† Department of Physics and the Center of Materials Research and Analysis, University of Nebraska–Lincoln, Lincoln, NE 68588-0111, USA

‡ Department of Physics and the Solid Science and Technology Program, Syracuse University, Syracuse, NY 13244-1130, USA

§ Department of Physics, University of Rhode Island, Kingston, RI 02881, USA

‖ Department of Physics and the Materials Science Program, University of Wisconsin–Madison, Madison, WI 53706, USA

Received 13 February 1995, in final form 26 June 1995

Abstract. Using angle-resolved photoemission and inverse photoemission, the electronic structure of films of the molecular icosahedron orthocarborane ($C_2B_{10}H_{12}$) on Cu(100) has been studied. The measured gap between the highest occupied molecular orbitals and the lowest unoccupied molecular orbitals is in good agreement with modified neglect of differential overlap calculations. An unoccupied exopolyhedral state has been found and is ascribed to molecular orbital hybridization. This hybridization is consistent with the observed dispersion of the orthocarborane molecular orbitals. This molecular orbital dispersion indicates a surface Brillouin zone edge with an average radius of 0.7 $Å^{-1}$, and suggests that the molecules adopt local close-packed ordering in the overlayers, with an intermolecular distance of 5.58 Å.

1. Introduction

The adsorption of thin molecular films on solid surfaces has been extensively investigated in recent years due to a general scientific interest and for their potential technological applications. The band-structure effects or binding-energy shifts (dispersion) of molecular-orbital-induced states are generally related to either local or long-range ordering in molecular films. Both crystalline and band structures have been detected for small molecules such as N_2 and CO on a variety of metal substrates [1–5]. For these small molecules, band dispersions as large as about 1 eV have been observed. For the large molecule C_{60}, it has been established that the electronic structures of both its solid and thin film forms are well described by band-structure calculations [6–10]. Although mapping the band structure experimentally has proved to be difficult, significant dispersion of both the conduction and valence bands has been found for C_{60} films on GeS(100) [11, 12].

Low energy electron diffraction (LEED) studies on C_{60} films of thicknesses less than two monolayers on Cu(111), Cu(100), and Cu(110) [16] have shown strong nearest-neighbour ordering of molecules, but lack of long range order. Long-range order was achieved after annealing of the films to 800 K. Epitaxial growth with two C_{60}(111) domains was achieved for thick films on Cu(100). Hexagonal close-packed layers were found for C_{60} on Au(111) [13], Au(100) [14], and Cu(111) [10, 15], using a scanning tunnelling microscope (STM), atomic force microscope (AFM), and x-ray diffraction. For C_{60} deposition on Au(100), a highly compressed C_{60} monolayer is incommensurate with the Au(100) substrate along the

0953-8984/95/367185+10$19.50

⟨110⟩ direction. The nearest-neighbour distance in the adsorbed layer is compressed by up to 20% of the van der Waals intermolecular spacing of solid C_{60} due to the deformation of charge density around the molecules and intermolecular bonding between them.

Orthocarborane (*close*-1,2-dicarbadodecaborane or $C_2B_{10}H_{12}$) is a cage molecule with the B_{12} icosahedral unit with a two-carbon substitution [17]. Similar to C_{60}, orthocarborane is highly stable, both chemically and physically, due to its closed cage structure. With respect to size, orthocarborane represents the middle ground between the smaller molecules such as CO and the larger molecules such as C_{60}. In this paper we present angle-resolved photoemission and inverse photoemission studies of the orthocarborane films on Cu(100).

2. Experiment

The photoemission experiments were carried out in an angle-resolved photoemission system equipped with a hemispherical electron energy analyser, as described in detail elsewhere [18]. The light source was dispersed by a 4 m normal incident monochromator at the Synchrotron Radiation Center in Stoughton, Wisconsin. The binding energies of the photoemission features are referenced to the Fermi energy of the clean Cu(100) surface. The energy resolution of the photoemission spectra, including the light source and the electron energy analyser, is about 60 meV. For the inverse photoemission studies, a Geiger–Müller detector with a SrF_2 window with a pass energy of 9.5 eV was used in conjunction with a Erdman-Zipf electron gun. The overall energy resolution was about 0.40 eV. All inverse photoemission spectra were collected with the electron gun at normal incidence and the detector positioned at 35° off the surface normal. The Fermi level was established from the clean, well ordered, Cu(100) substrate. The substrate surface was cleaned prior to each run by Ar^+ ion sputtering and subsequent annealing at 850 K. The purity of the orthocarborane compound was greater than 98% and a detailed description for the preparation of the orthocarborane has been described elsewhere [19].

3. Electronic structure in the adsorbed phase

Figure 1 presents a sequence of both photoemission electron spectroscopy (PES) and inverse photoemission electron spectroscopy (IPES) spectra of orthocarborane adsorbed on Cu(100) as a function of film thickness. The PES and IPES spectra for one monolayer of orthocarborane adsorbed onto Cu(100), compared with the modified neglect of the differential overlap (MNDO) calculation of orbital energies for free orthocarborane molecules, are shown in figure 2. As has been noted in previous work [20], the similarity in the occupied-orbital structure of the spectra for both adsorbed and gaseous phases demonstrates that the orthocarborane is adsorbed molecularly on Cu(100) at 180 K. From studies of the light polarization dependence, discussed in detail elsewhere [20], the molecular alignment for a molecular monolayer has been determined. The shifts of the $6a_1$ and $3b_2$ molecular orbitals to greater binding energies and $8a_1$ orbital to smaller binding energies have allowed us to propose a specific bonding orientation [20]. This molecular adsorption occurs with a preferential bonding orientation in which the two carbon atoms in the molecule bond to the surface and the molecular axis is parallel with the surface normal, as schematically shown in figure 3. A C_{2v} symmetry is preserved with a molecular axis from the C_1–C_2 bond through the cage to the B_9–B_{12} bond. As seen in figure 1 and 2, the occupied Cu 3d bands, the unoccupied s–p band, and the image state (~4.35 eV) of Cu substrate are suppressed with adsorption of orthocarborane. The orthocarborane induced occupied states

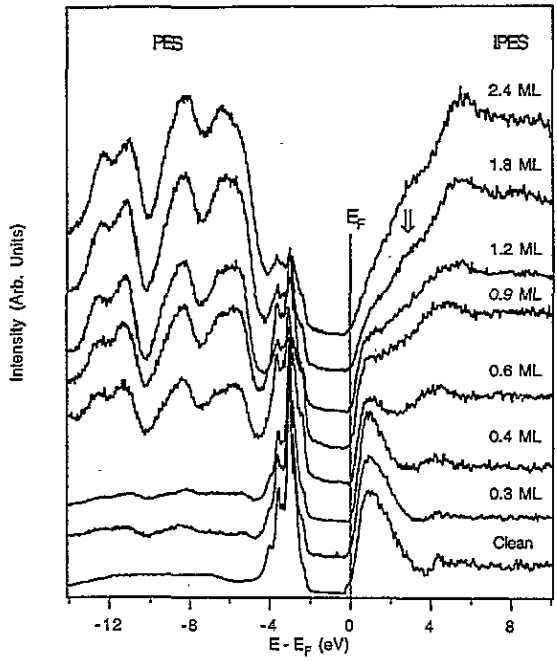

Figure 1. Normal-emission photoemission and normal-incidence inverse photoemission spectra of orthocarborane on Cu(100) at 180 K as a function of orthocarborane coverage. The photoemission spectra were acquired with a photon energy of 30 eV.

are seen at about 5.7, 6.5, 8.5, 11.2 and 12.5 eV below the Fermi energy. A molecular-induced feature is also seen at an energy of 5.1 eV above the Fermi level. These features can be properly assigned to the molecular orbitals on the basis of the MNDO semiempirical molecular orbital calculations [17, 21]. The 6.5 and 12.5 eV features below E_F are due to the emissions from the $8a_1$ and $5a_1$ molecular orbitals respectively. The features at 8.5 eV (due to $4b_1$, $4b_2$, and $7a_1$ orbitals) and 11.2 eV (due to $3b_1$, $3b_2$, and $6a_1$ orbitals) below E_F are combinations of molecular orbitals but the majority of their weight is from b_1 and b_2 molecular orbitals. The 5.7 eV feature below E_F is a more complex mixture of a_1, a_2, b_1, and b_2 molecular orbitals. The 5.1 eV unoccupied feature can be assigned to the mixture of molecular orbitals with both a and b symmetry ($7b_{1,2}$, $8b_{1,2}$, $11a_1$ and $12a_1$).

4. Evolution of HOMO and LUMO states

As shown in figure 1, both the highest occupied molecular orbitals (HOMO) and the lowest unoccupied molecular orbital (LUMO) states shift away from the Fermi level, while simultaneously becoming more highly resolved, with increasing coverage. In figure 4 we have plotted the energy of the HOMO and LUMO states, relative to the substrate Fermi level, as a function of coverage. We again see that as the film coverage increases the HOMO and LUMO diverge from one another, with the HOMO shifting to higher binding energies and the LUMO towards the vacuum. These shifts do not follow the changes in the work function and therefore are not due to changes in the surface potential. If we consider band bending (an initial-state effect) we would expect the energies of both the HOMO and the LUMO, relative to the Fermi level, to rigidly shift in the same direction. Since the HOMO and the LUMO symmetrically diverge from one another, and the Fermi level, we can rule

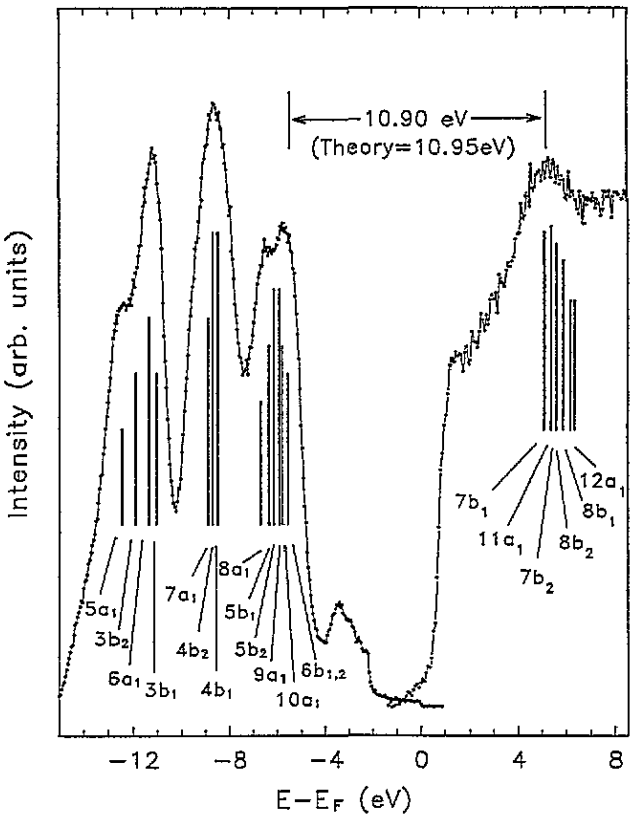

Figure 2. Normal-emission photoemission and normal-incidence inverse photoemission spectra of one molecular orthocarborane monolayer on Cu(100) at 180 K, compared with clean Cu(100). Light with 25 eV photon energy was used for the photoemission. The corresponding molecular orbitals from MNDO theoretical calculations are indicated.

out band bending and charge transfer initial-state effects.

These symmetric, but opposite, shifts of the HOMO and LUMO states with increasing coverage can be understood in terms of the influence of the Cu(100) substrate. Such shifts have also been observed with increasing C_{60} coverage on a variety of substrates [22], as well as alkane molecular films [23]. As with orthocarborane, the majority of the shifts of the molecular orbital binding energies take place during the adsorption of the first two molecular layers. Such symmetric shifts away from the Fermi level of both the occupied and unoccupied states are characteristic of final-state effects, as has been observed in the shallow 4f core levels of rare earths [24]. It is difficult to invoke initial-state effects when the molecular orbitals of the orthocarborane are only slightly perturbed upon condensation.

As seen in figure 4, the observed energies of both the LUMO and HOMO states of the thick molecular films, relative to the Fermi level, are in excellent agreement with the theoretical MNDO calculations [17, 21] and with gas phase measurements [25]. The MNDO calculations of the orbital energies are offset from the experimentally determined values of the condensed phase by approximately 7 eV. This difference between the isolated free cluster and the condensed film can be accounted for in terms of the work function of the orthocarborane/Cu(100) system [20], and does not appear to require appreciable inclusion of other solid state effects.

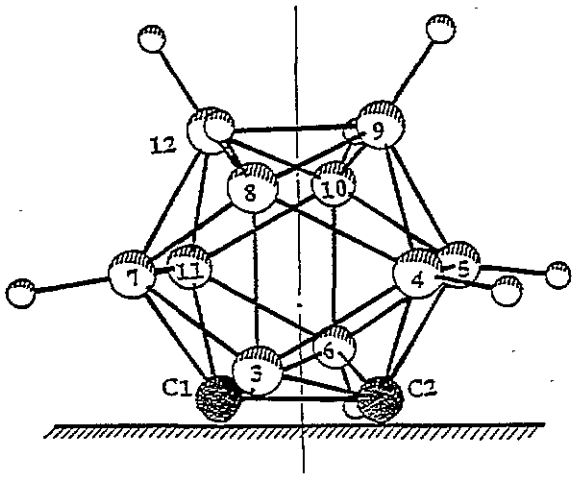

Figure 3. A schematic presentation of the minimum energy MNDO structure for $C_2B_{10}H_{12}$ [20] and its preferential orientation of orthocarborane adsorption on Cu(100). The dashed line is the molecule axis of C_{2v} symmetry.

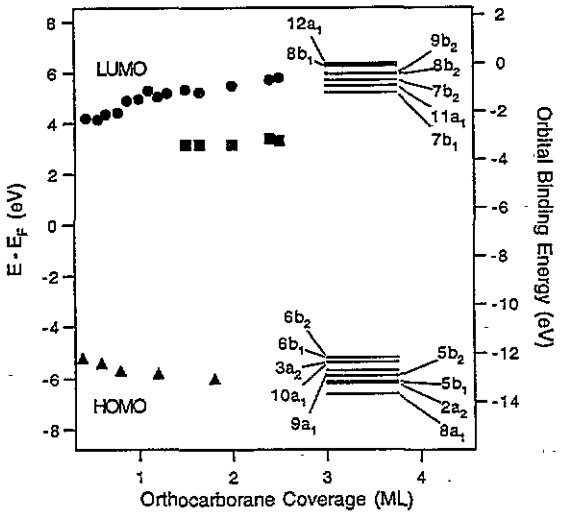

Figure 4. The binding energies of the HOMO (▲), the LUMO (●), and the exopolyhedral state (■) of orthocarborane on Cu(100), referenced to the substrate Fermi level, as a function of orthocarborane coverage. Included are the HOMO and LUMO molecular orbital energies of the free molecules which have been derived from MNDO calculations [7, 8].

From our results in figure 4, we see that the band gap is largely determined by the molecular HOMO–LUMO gap. In spite of the resemblance of the molecular orbitals of orthocarborane to C_{60}, *i.e. in* π*-orbital character, the Fermi energy is very nearly midgap,* in contrast to C_{60} where the Fermi energy is just below the LUMO (the conduction band minimum) [26, 27]. The agreement between the MNDO calculation of the HOMO–LUMO gap of the free molecule and the experimental value for the orthocarborane molecular icosahedra film are better than the predicted HOMO–LUMO gap by some theories for C_{60} [28].

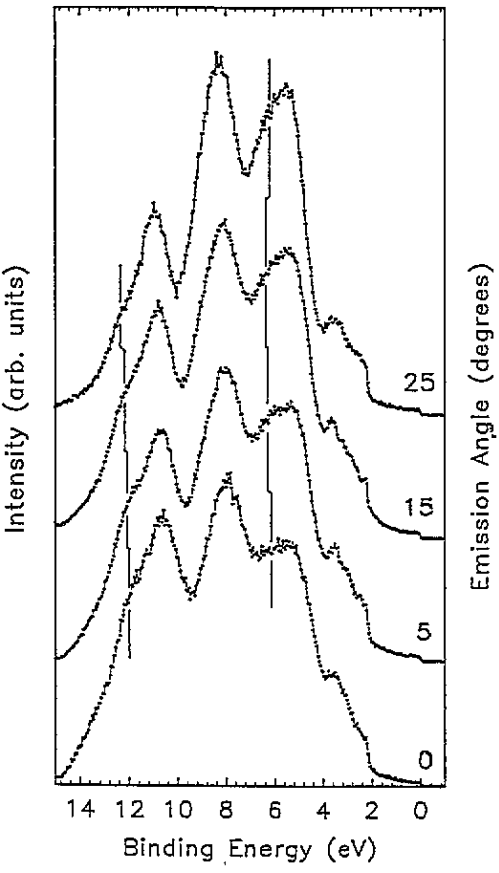

Figure 5. Angle-resolved photoemission spectra as function of electron emission angle for 8 L orthocarborane on Cu(100) at 180 K. The photon energy was 25 eV and incident at an angle of 42°.

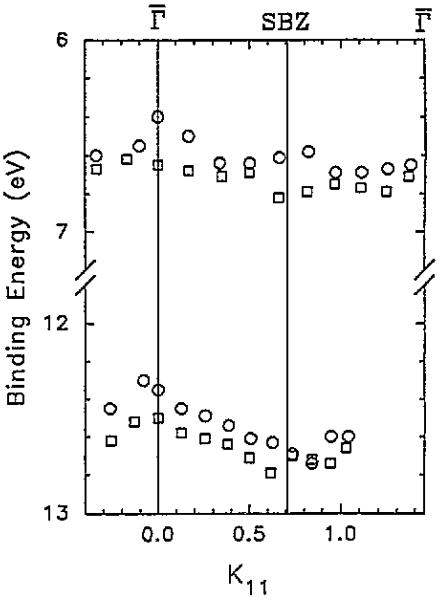

Figure 6. Dispersion of the molecule-induced 6.5 and 12.5 eV bands for 8 L (○) and 16 L (□) of orthocarborane on Cu(100) at 180 K. p-polarized light with a photon energy of 25 eV was used.

5. Molecular orbital hybridization

At the onset of multilayer growth a weak state appears within the HOMO–LUMO gap at approximately 3.2 eV above the Fermi level, as indicated in figure 1. This inverse photoemission feature does not shift with increasing orthocarborane coverage as shown in figure 4. Since there is no counterpart to this state in the molecular orbitals of orthocarborane, we must conclude that it is exopolyhedral and possibly an extramolecular state. This state could arise from defects, molecular misorientation, or from the loss of exopolyhedral hydrogen. An alternative possibility is an extrinsic state arising from molecule–molecule hybridization.

The behaviour of this exopolyhedral state with annealing, or changing coverages, does not support the conjecture that it is attributable to excess disorder within the films. This exopolyhedral state has not been observed for thick films nor does it appear until the onset of multilayer growth. The exopolyhedral state persists beyond a few monolayers provided the growth rate is slow. Only when thick films are grown at high growth rates

is the exopolyhedral state absent from the IPES spectra. If thick films are annealed at low temperatures (250 K), the exopolyhedral state returns, while the LUMO density of states is left largely unperturbed. Clearly this state can only exist for uniform films and it may be attributed to the hybridization of molecular orbitals.

The absence of this state in the molecular monolayer films suggests that the overlayer film is strongly screened by the Cu(100) substrate. If this state is indeed extrinsic in origin, the effect of damping by the substrate is to screen nearest-neighbour interactions. Only until a multilayer film is established (~1.5 ML) does screening by the substrate become insufficient to dampen out this exopolyhedral state and it is observed at about 3.2 eV in the IPES spectra. Similar states have not been reported for other clusters like C_{60}, except in their doped phases. If this state for orthocarborane is a result of extramolecular orbital hybridization, it would suggest that the formation of bands from the molecular orbitals is possible. Such band structure has been observed, as will be discussed below.

6. Band structure effects

A selected sequence of the angle-resolved photoemission spectra for one monolayer of orthocarborane on Cu(100) at 180 K is shown in figure 5. The orthocarborane-induced features exhibit small shifts in binding energy with increasing emission angle. Proper dispersion analysis requires that we take into account the binding energy shift as a result of light- and electron-induced decomposition of the molecularly adsorbed orthocarborane, as discussed in detail in [29]. The light-induced decomposition results in a general decrease in the binding energies and a slight broadening of the molecular orbitals. This occurs because a p-type boron carbide is eventually formed from the decomposition of the orthocarborane. Since all the features induced by the molecular orbitals in the photoemission spectra taken at various times resemble each other, and are similar to the ones measured for gas phase, it is reasonable to assume that the orthocarborane films are only slightly affected by light and that the films retain their molecular character. To ensure a proper subtraction of the light-induced effect from the intrinsic dispersion, binding energy shifts versus photon exposure time were analysed, and an exponential decrease of binding energies with photon exposure time was found and has been taken into account.

The admixture of molecular orbitals with different symmetry characters in the features at 5.7, 8.5, and 11.2 eV (at normal emission) makes it difficult to identify, unequivocally, the dispersion of an individual molecular orbital. There is also great difficulty in accounting for the changes in the cross-sections with emission angle, for the various molecular orbitals with different symmetries which contribute to these photoemission features. The dispersions of the 6.5 eV ($8a_1$) and 12.5 eV ($5a_1$) bands provide the clearest indication of band structure. As shown in figure 6, the 6.5 eV and 12.5 eV bands exhibit dispersion with $k_\parallel$. One of these bands, corresponding to the $5a_1$ molecular orbital, clearly disperses to higher binding energies with increasing $k_\parallel$.

While dispersion of a fully symmetric orbital (a_1) to higher binding energies with increasing $k_\parallel$ is unusual, the dispersion of this band reflects the wave function of this orbital and perhaps the local bonding geometry of orthocarborane molecules. An orientation of molecules so as to achieve an antibonding configuration (at $\bar{\Gamma}$ or normal emission) of this orbital among adjacent molecules is postulated. This permits the observed dispersion to occur, instead of the normally expected dispersion to smaller binding energies away from $\bar{\Gamma}$. The qualitative dispersion observed with these films of molecular icosahedra is similar to that observed with C_{60} [12], i.e. increasing binding energies with increasing $k_\parallel$. There are also similarities with other molecular films, for example C_2H_4 and C_6H_6 [30]. For C_2H_4

and C_6H_6, dispersion is not always observed into the second Brillouin zone, particularly for hexagonal packing structure. The hexagonal packing of orthocarborane would explain the difficulty we have had in observing dispersion in the second Brillouin zone as well as the negative dispersion for the $5a_1$ orbital in this adsorbate.

Within our experimental resolution, these dispersions are more obvious when the analyser scans in the plane defined by the light vector potential and the surface normal (even geometry) than when the analyser scans along the direction which is perpendicular to plane defined by the vector potential. Such differences in the dispersions for the different $k_{\parallel}$ directions should be related to the difference in symmetry, and corresponding changes in relative cross-section.

The small but significant dispersion of the bands resulting from the hybridization of molecular orbitals provides evidence of the existence of some ordering within the adsorbed orthocarborane films. As seen in figure 6, the surface Brillouin zone edge is at 0.7 Å^{-1}. This is different from any Brillouin zone that involves the substrate and suggests that the interaction between the molecule and Cu(100) substrate is weak [31]. A hexagonal close-packed structure is a likely structure within the small ordered domains expected for the orthocarborane overlayer. Assuming local ordering of the overlayer in this configuration, the size of Brillouin zone obtained from our photoemission results suggests that the intermolecular distance is 5.58 Å. This distance is very close to the size of the free orthocarborane molecule (with a diameter of 5.6 Å).

A similar amplitude for the dispersion and approximately the same size for surface Brillouin zone are found for both 8 Langmuir and 16 Langmuir films (as seen in figure 4). Since one monolayer corresponds to 8–10 Langmuir orthocarborane exposure [20], the Brillouin zone observed at 16 Langmuirs is an average effect of both the first layer and the second layer. The equivalent sizes for the surface Brillouin zone indicate that the second layer of orthocarborane grows in close registry with the first layer.

While the dispersion of the molecular orbitals suggests that there is a local ordering in the molecular films, there is no clear indication of long-range order for the orthocarborane overlayers, either by low-energy electron diffraction (LEED), or by atomic beam scattering (ABS) experiments [20]. In the case of C_{60} deposition on Au(111), LEED also fails to provide any indication of diffraction pattern indicative of long-range order, even though the STM images and x-ray diffraction data reveal an ordered overlayer. Unfortunately, due to the low resolution of IPES, relative to the PES, no dispersion was observed for the LUMO states.

7. Summary

In conclusion, we observed that the HOMO–LUMO gap and the electronic structure of the adsorbed molecular orthocarborane films are in good agreement with the MNDO calculations and are similar to those of the free molecules. Such similarity confirms that the orthocarborane adsorbs molecularly and is weakly bonded on the Cu surface at 180 K. We found evidence of band formation for the condensed films from the molecular orbitals with a1 symmetry. The molecules not only have a preferential bonding orientation but also exhibit short-range order when adsorbed on the surface. Both the existence of the exopolyhedral state and the band dispersion of the occupied molecular orbitals indicate that weak intermolecular hybridization occurs within the orthocarborane overlayer.

Acknowledgments

This work was funded by NSF through grants DMR92-21655, DMR94-96131 and DMR91-19735. The authors would like to thank Jian Ma, R J Kelley and the staff of the Synchrotron Radiation Center at Stoughton, Wisconsin, for technical assistance. The Synchrotron Radiation Center is supported by the NSF.

References

[1] Dowben P A, Sakisaka Y and Rhodin T N 1984 *Surf. Sci.* **147** 89
[2] Freund H-J, Eberhardt W, Heskett D and Plummer E W 1983 *Phys. Rev. Lett.* **50** 768
[3] Kuhlenbeck H, Saalfeld H B, Buskotte U, Neumann M, Freund H-J and Plummer E W 1989 *Phys. Rev.* B **39** 3475
Heskett D, Plummer E W and Messmer R P 1984 *Surf. Sci.* **139** 558
[4] Memmel N, Rangelov G, Bertel B, Dose V, Kometer K and Rüsch N 1989 *Phys. Rev. Lett.* **63** 1884
[5] Greuter F, Heskett D, Plummer E W and Freund H-J 1983 *Phys. Rev.* B **27** 7117
[6] Satio S, Ashiyama A, Saito S, Hamada N and Miyamoto Y 1992 *J. Phys. Chem. Solids* **53** 1475
[7] Weaver J H, Martins J L, Komada T, Chen Y, Ohno T R, Kroll G H and Troullier N 1991 *Phys. Rev. Lett.* **66** 1741
[8] Jost M B, Troullier N, Poirier D M, Martins J L and Weaver J H 1991 *Phys. Rev.* B **44** 1966
[9] Y. Kawazoe, Kamiyama H, Maruyama Y and Ohno K 1993 *Japan. J. Appl. Phys.* **32** 1433
[10] Hashizume T, Motai K, Wang X D, Shinohara H, Saito Y, Maruyama Y, Ohno K, Kawazoe Y, Nishina Y, Pickering H W, Kuk Y and Sakurai T 1993 *Phys. Rev. Lett.* **71** 2959
[11] Themlin J-M, Bouzidi S, Coletti F, Debever J-M, Gensterblum G, Thiry P A and Pireaux J-J 1993 *Appl. Surf. Sci.* **65/66** 76
[12] Gensterblum G, J-J Pireaux J-J, Thiry P A, Caudano R, Buslaps T, Johnson R L, Le Lay G, Aristov V, Günther R, Taleb-Ibrahimi, Indlekofer G and Petroff Y 1993 *Phys. Rev.* B **48** 14 756
Benning P J, Olson C G, Lynch D W and Weaver J H, 1994 *Phys. Rev.* B **50** 11 239
[13] Zhang Y, Cao Z and Weaver M J, 1992 *J. Phys. Chem.* **96** 510
Altman E I and Colton R J 1992 *Surf. Sci.* **279** 49
[14] Kuk Young, Kim D K, Suh Y D, Park K H, Noh H P, Oh S J, and Kim S K 1993 *Phys. Rev. Lett.* **70** 1984
[15] Motai K, Hashizume T, Shinohara H, Saito Y, Pickering H W, Nishina Y and Sakurai T 1992 *Japan. J. Appl. Phys.* **32** L450
[16] Rowe J E, Rudolf P, Tjeng L H, Malic R A, Meifs G and Chen C T 1992 *Int. J. Mod. Phys.* B **6** 3909
[17] Lee Sunwoo, Dowben P A, Wen A T, Hitchcock A P, Glass J A Jr and Spencer J T 1992 *J. Vac. Sci. Technol.* A **10** 881
[18] Dowben P A, LaGraffe D and Onellion M 1989 *J. Phys.: Condens. Matter* **1** 6571
[19] Hitchcock A P, Wen A T, Lee Sunwoo, Glass J A Jr, Spenser J T and Dowben P A 1993 *J. Phys. Chem.* **97** 8171
[20] Zeng H, Byun D, Zhang J, Vidali G, Onellion M and Dowben P A 1994 *Surf. Sci.* **313** 239
[21] Byun Donjin, Lee Sunwoo, Hu Y-F, Bancroft G M, Hwang S-D, Glass J A, Zhang Jiandi, Spencer J T, Jian Ma and Dowben P A 1994 *J. Electron Spectroc. Relat. Phenom.* **69** 111
Guest M F and Hillier I H 1973 *Mol. Phys.* **26** 435
Dewar M J S and McKee M 1980 *Inorg. Chem.* **19** 2662
Chung C-C, Beaudet R A and Segal G A 1970 *J. Am. Chem. Soc.* **92** 4158
[22] Chase S J, Basca W S, Mitch M G, Pilione L J and Lannin J S 1992 *Phys. Rev. B* **46** 7873
Ohno T R, Chen Y, Harvey S E, Kroll G H, Benning P J and Weaver J H 1991 *Phys. Rev.* B **44** 13 747
Maxwell A J, Brühwiler P A, Nilsson A, Mtensson N and Rudolf P 1994 *Phys. Rev.* B **49** 10 717
[23] Linge R L, Padowitz D F, Jordan R E, McNeill J D and Harris C B 1994 *Phys. Rev. Lett.* **72** 2243
[24] Ortega J E, Himpsel F J, Li Dongqi and Dowben P A 1994 *Solid State Commun.* **91** 807
Fedorov A V, Arenholz E, Starke K, Navas E, Baumgarten L, Laubschat C and Kaindl G 1994 *Phys. Rev. Lett.* **73** 601
[25] Brint P, Sangchakr B, McGrath M, Spalding T R and Suffolk R J 1990 *Inorg. Chem.* **29** 47
[26] Lof R W, van Veenendaal M A, Koopmans B, Jonkman H T, and Sawatzky G A 1992 *Phys. Rev. Lett.* **68** 3924
De Seta M and Evangelisti F 1993 *Phys. Rev. Lett.* **71** 2477

[27] Takahashi T, Suzuki S, Morikawa T, Katayama-Yoshida H, Hasegawa S, Inokuchi H, Seki K, Kikuchi K, Suzuki S, Ikemoto K and Achiba Y 1992 *Phys. Rev. Lett.* **68** 1232
[28] Siato S and Oshiyama A 1991 *Phys. Rev. Lett.* **66** 2637
[29] Byun D, Hwang Seong-don, Zhang Jaindi, Zeng H, Perkins F K, Vidali G and Dowben P A 1995 *Japan. Appl. Phys. Lett.* **35** L941
[30] Steinrück H-P 1994 *Appl. Phys.* A **59** 517
Huber W, Zebisch P, Bornemann T and Steinrück H-P 1991 *Surf. Sci.* **258** 16
Steinrück 1994 *Vacuum* **45** 715
[31] Dowben P A, Kime Y J, Hutchings C H, Li Wei and Vidali G 1990 *Surf. Sci.* **230** 113